Hydrol. Earth Syst. Sci., 16, 4571–4579, 2012
www.hydrol-earth-syst-sci.net/16/4571/2012/
doi:10.5194/hess-16-4571-2012

Hydrology and Earth System Sciences

Hydrogeological settings of a volcanic island (San Cristóbal, Galapagos) from joint interpretation of airborne electromagnetics and geomorphological observations

A. Pryet[1], **N. d'Ozouville**[1], **S. Violette**[1], **B. Deffontaines**[2], **and E. Auken**[3]

[1]UPMC, Université. Paris 6 – CNRS, Sisyphe, 4 place Jussieu, 75252 Paris, cedex 05, France
[2]UPE, GTMC Laboratory, Marne-La-Vallée, France
[3]University of Arhus, Department of Earth Sciences, HydroGeophysics Group, Høegh-Gulbergs gade 2, 8000 Arhus, Denmark

Correspondence to: A. Pryet (a.pryet@gmail.com)

Received: 6 August 2012 – Published in Hydrol. Earth Syst. Sci. Discuss.: 21 August 2012
Revised: 13 November 2012 – Accepted: 15 November 2012 – Published: 4 December 2012

Abstract. Many volcanic islands face freshwater stress and the situation may worsen with climate change and sea level rise. In this context, an optimum management of freshwater resources becomes crucial, but is often impeded by the lack of data. With the aim of investigating the hydrogeological settings of southern San Cristóbal Island (Galapagos), we conducted a helicopter-borne, transient electromagnetic survey with the SkyTEM system. It provided unprecedented insights into the 3-D resistivity structure of this extinct basaltic shield. Combined with remote sensing and fieldwork, it allowed the definition of the first hydrogeological conceptual model of the island. Springs are fed by a series of perched aquifers overlying a regional basal aquifer subject to seawater intrusion. Dykes, evidenced by alignments of eruptive cones at the surface, correspond to sharp sub-vertical contrasts in resistivity in the subsurface, and impound groundwater in a summit channel. Combined with geomorphological observations, airborne electromagnetics are shown to be a useful for hydrogeological exploratory studies in complex, poorly known environments. They allow optimal development of land-based geophysical surveys and drilling campaigns.

1 Introduction

With increasing population and limited resources, freshwater supply has become a critical issue for many volcanic islands (Falkland and Custodio, 1991; Falkland, 1999). Climate change will most probably be associated with rising temperature and increasing sea level (IPCC, 2007), which can reduce groundwater recharge and intensify seawater intrusion (Falkland, 1999; Underwood et al., 1992). In this context, there is a need for a sustainable management of freshwater resources, which can only be achieved once aquifers are clearly delineated and their interactions with the ocean are sufficiently understood, which is not often the case.

Conditions of groundwater occurrence are often clearly defined in well-studied islands, where human development has been historically accompanied with the drilling of numerous galleries and boreholes such in the Canary and Hawaiian Islands (Custodio, 2004; Gingerich and Oki, 2000). But the hydrogeological settings are poorly constrained in many other islands where human development is more recent, such as the Galapagos Archipelago (d'Ozouville, 2007a). On these islands, there are few or no drill holes and groundwater monitoring is sparse or nonexistent.

Volcanic islands present peculiar hydrogeological characteristics inherited from their specific geological structure. The bulk of volcanic edifices is composed by lava flows and tephra deposits, which are intruded by dykes in vent zones (Bardintzeff and McBirney, 2006). Dykes can form impervious sub-vertical barriers to groundwater flow, while red "baked" soils and tuff deposits may form impervious layers sub-parallel to the topography (Custodio, 2004; Singhal and Gupta, 2010).

Geophysics has successfully contributed to groundwater characterization of volcanic environments, in particular with

electrical, electromagnetic, and audiomagnetotelluric methods (Aizawa et al., 2009; Descloitres et al., 2000; Gómez-Ortiz et al., 2007; Lénat et al., 2000; Lienert, 1991; MacNeil et al., 2007; Revil et al., 2004). Yet, the development of land-based surveys is often long and costly over large, inaccessible areas. Airborne Electromagnetics (AEM) can now tackle the issue and cover extensive study areas in a short lapse of time. Several systems have been developed, measuring in the frequency-domain such as Resolve and DigHEM by Fugro Airborne Surveys (e.g. Mullen et al., 2007 and Siemon, 2009), and in the time-domain, such as SkyTEM (Sørensen and Auken, 2004) or VTEM by Geotech Airborne Inc. AEM surveys have been successfully conducted during the past decades for risk assessment and hydrogeological prospection in various geological contexts (Bosch et al., 2009; Mogi et al., 2009; Steuer et al., 2009; Supper et al., 2009; Viezzoli et al., 2010b), including volcanic (Auken et al., 2009b; Finn et al., 2001, 2007; d'Ozouville et al., 2008). In most of the above-mentioned studies, geophysical data have been interpreted with a substantial set of drill hole and geological data available prior to the survey.

The project Galapagos Islands Integrated Water Studies (GIIWS) was initiated in 2003 with the aim of conducting studies in hydrology and promoting a sustainable management of water resources in the Archipelago. Within the framework of the GIIWS project, an extensive SkyTEM exploratory survey was conducted in 2006 over the islands of Santa Cruz and San Cristóbal. Here, we first describe a newly acquired geomorphological dataset collected on the Island of San Cristóbal from remote sensing and field work. The AEM geophysical data collected on this island is then presented in 3-D with a newly available interpolation method (Pryet et al., 2011), and a joint interpretation is performed with the geomorphological dataset. From this analysis, the first hydrogeological conceptual model of the island is proposed. Finally, we discuss the hydrogeological implications and issues related to groundwater characterization based on resistivity mapping in volcanic contexts.

2 Study area

2.1 Geology

San Cristóbal is a basaltic island located on the Nazca oceanic plate, at the eastern end of the Galapagos Archipelago. The island has an elongated shape, 50 km long in the SW–NE direction and 14 km in SE–NW, for a total surface of 558 km^2. It can be divided into an older southwestern sub-region where volcanic activity coalesced to form a major shield culminating at 710 m a.s.l. (above sea level), and a younger flat and arid sub-region to the northeast (Geist et al., 1986). This study focuses on the older, inhabited southwestern part, where permanent springs and streams are present (Figs. 1 and 2).

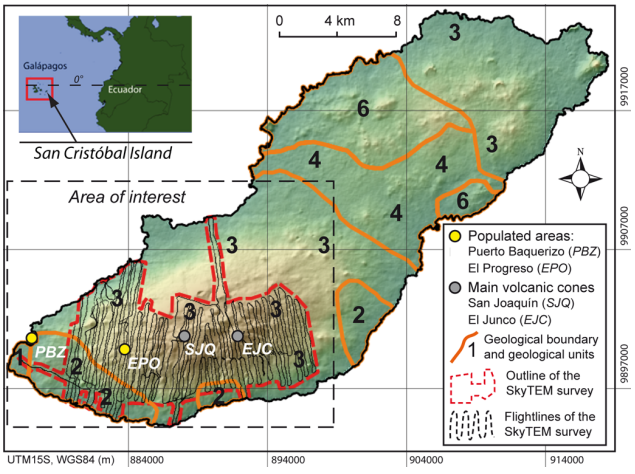

Fig. 1. Geographical settings of San Cristóbal Island. Shaded relief map from the SRTM digital elevation model (Rabus et al., 2003). Geological boundaries from Geist et al. (1986), with ages from the older (1, 2.3 Ma) to younger (6, historical) formations. Age 2 are reversely polarized flows (> 0.78 Ma) and age 3 to 6 are normally polarized (< 0.78 Ma).

Reversely polarized flows of the Matuyama epoch (> 0.78 Ma) outcrop at the base of the southwestern shield (Age 2, Fig. 2), but most of the volcano is covered by younger lava flows of the subsequent Bruhnes epoch (Age 3, Fig. 2) (Cox, 1971). Eruptions were relatively continuous and characterized by moderately thick (1 to 3 m) *pahoehoe* and *aa'* flows (Geist et al., 1986), locally interbedded with red "baked" soils (d'Ozouville, 2007b). Pyroclastic material forms an exceedingly small part of the volume of the volcano, but at least 10 m of tephra was deposited over the entire summit during the culminating eruptions some 600 000 yr ago (Geist et al., 1986). Few dykes naturally outcrop on San Cristóbal, but their position may be inferred from their superficial expressions: eruptive fissures and cones. When cones are elongated or aligned, they are likely to reveal the presence of dyke swarms (Acocella and Neri, 2009; Chadwick and Howard, 1991).

A comprehensive map of volcanic cones and surface lineaments was completed from the geomorphological map provided by Ingala, Orstom and Pronareg (1987), Google Earth® images and the Shuttle Radar Topography Mission (SRTM DEM) (Rabus et al., 2003) (Fig. 2). We observe that cones do not align along a single rift zone, but are organized along two major volcanic alignments WSW–ENE trending and form an elongated ellipsoid at the summit. To the north, eruptive cones are locally aligned with antithetic normal faults, which suggests the intrusion by dykes. The NNW–SSE extensional tectonic stress that controlled the position of the main eruptive zones is likely to be at the origin of the WSW–ENE trending faults.

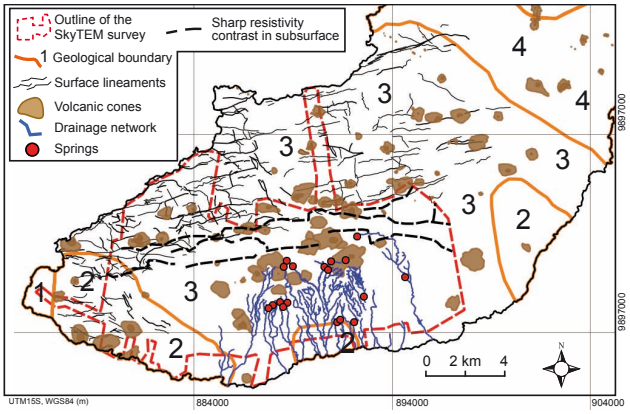

Fig. 2. Surface morphology of the southwestern shield of San Cristóbal island. Geological boundaries from Geist et al. (1986), see caption of Fig. 1 for details. Drainage network, surface lineaments and volcanic cones were mapped from the Google Earth® SPOT imagery and SRTM DEM. Black dashed lines underline major resistivity offsets in the 3-D geophysical model (Fig. 5).

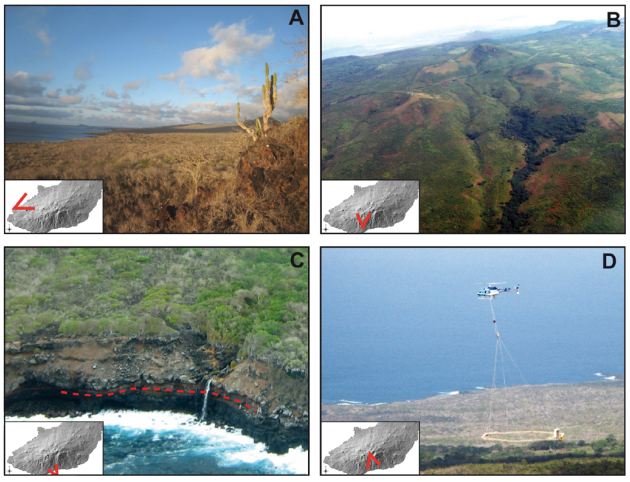

Fig. 3. Photographs of the southern shield of San Cristóbal Island. **(A)** The dry leeward slopes covered by shrubs and cactus. **(B)** San Joaquin volcanic cone, the topography is incised by streams fed by springs. **(C)** Perched stream over a red "baked" soil layer (underlined with a red dashed line). **(D)** The helicopter carrying a frame with the SkyTEM transmitter and receiver coils. Photographs GIIWS project.

2.2 Climate

The climate of the Galapagos Islands is relatively dry with respect to its equatorial location (Colinvaux, 1972). Rainfall at low elevation is particularly weak, with a median annual total of 343 mm (1950–2005, INHAMI) at Puerto Baquerizo (6 m a.s.l.). There is a marked contrast between the southern slopes exposed to the southeast trade-winds where vegetation is abundant, and the northern drier slopes covered by spiny shrubs and cactuses (Ingala, Orstom and Pronareg, 1987) (Fig. 3a, b). With the humid conditions prevailing in the highlands during the fog *garúa* season, the tephra deposits at the summit of San Cristóbal Island were rapidly weathered to form a thick, poorly permeable soil cover (Adelinet et al., 2008; Geist et al., 1986).

Only short-term climatic records are available in the highlands, but the climate of San Cristóbal is expected to share common patterns with the neighbouring better-studied Santa Cruz Island (Trueman and d'Ozouville, 2010). On the windward side, the rainfall orographic gradient was estimated to ca. 415 mm yr^{-1} per 100 m elevation from the coast up to the elevation of 440 m a.s.l. (d'Ozouville, 2007b; Pryet et al., 2012). On the basis of these values, the median annual total along the windward side of San Cristóbal is estimated to 1580 mm (Pryet, 2011).

2.3 Springs and streams

The mapping of the drainage network provided by Ingala, Orstom and Pronareg (1987) was improved and completed with air photographs and the high resolution images available on Google Earth®. The topography of southern San Cristóbal is incised by numerous ravines, many of which are dry (Fig. 3b). Intense rainfall events, particularly severe during El Niño years, lead to surface runoff with strong erosional power. On the central southern windward slope, the concentration of ravines is the densest and streamflow is fed by perennial springs. Due to infiltration losses through riverbeds, streamflow can decrease downstream and some of the rivers dry before reaching the ocean (Adelinet, 2005; d'Ozouville, 2007b). At least six streams reach the sea on a nearly permanent basis (Fig. 3c), which is a unique feature in the Galapagos Archipelago. Nevertheless, a majority of these rivers may dry during extreme dry periods associated with La Niña events (D. Geist, personal communication, 2012).

Springs were mapped with a GPS receiver to obtain a near-comprehensive map of major springs (Adelinet, 2005) (Fig. 2). Springs are located at slope breaks (depression springs) or at the outcropping of impermeable layers such as red "baked" soil (contact springs) (Fetter, 1994). Springs are poorly mineralized, with electrical conductivities ranging between 30 and 170 µS cm^{-1} (Adelinet, 2005). No hydrothermal activity is reported on the island; only traces of extinct fumaroles with white deposit (sodium sulfate) can be identified (Simkin, 1984).

3 Airborne electromagnetic survey

3.1 Data acquisition and processing

The airborne electromagnetic survey was conducted in May 2006 with the SkyTEM system (Sørensen and Auken, 2004)

(Fig. 3d). The average flight speed was 45 km h^{-1} and the flight altitude of the rig was 35–45 m above the ground surface. About 23 000 soundings were performed in 4 days along 900 km of flight lines, with a sounding every 25–50 m. Flight lines were generally oriented N–S with a spacing of 200 m (Fig. 1). The survey focused on the southern windward slopes, but a few lines were flown cross-island to obtain a full picture of the fresh-saltwater interface.

The system transmits two magnetic moments, a low moment for the resolution of the near surface layers and a high moment for the resolution of the deeper layers. The data filtering is designed to enhance near-surface resistivity variations by avoiding any smoothing of the early-time data, while late-time data are more severely filtered to obtain as much penetration depth as possible (Auken et al., 2009a).

Soundings were inverted to 4-layer 1-D vertical resistivity models with the spatially constrained inversion scheme (SCI) (Viezzoli et al., 2008, 2010a). With this method, local resistivity models are constrained by neighbouring soundings. This enhances the resolution of model parameters (i.e. layer resistivities and interfaces), which are not well resolved in an independent inversion. The inversion models were then interpolated to form a coherent 3-D grid of resistivity with the methodology detailed by Pryet et al. (2011). To obtain a finite 3-D model, the thickness of the last layer was arbitrarily fixed to 2.5 times the thickness of the overlying 3rd layer. The 3-D grid of resistivity was then imported into Paraview®, which allowed flexible visualization and volume extraction based on resistivity thresholds.

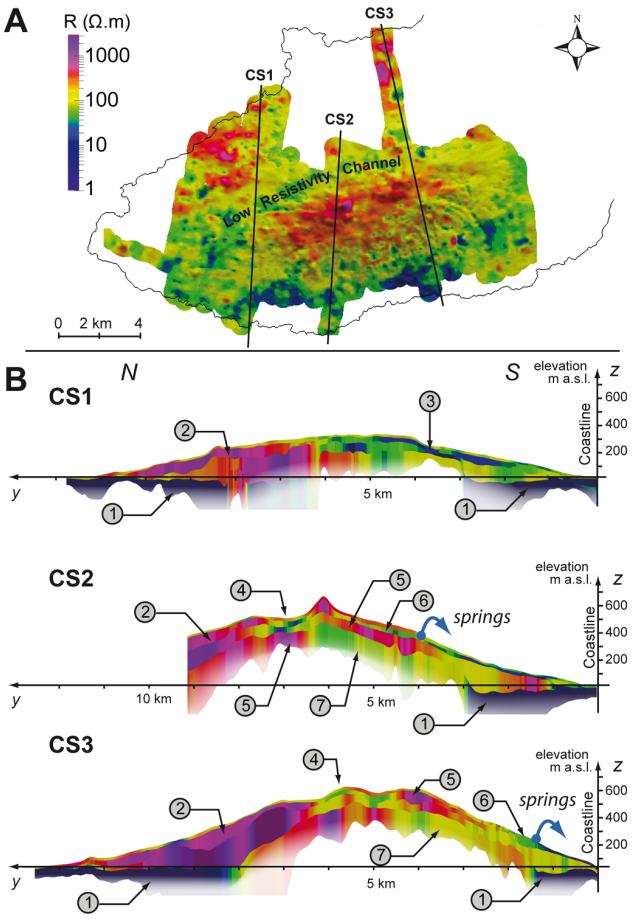

Fig. 4. (A) Surface resistivity of the 4-layer SkyTEM resistivity model. **(B)** Corresponding cross-sections. (1) Seawater intrusion (< 15 Ω m), (2) undifferentiated, unweathered, unsaturated volcanic rocks (> 400 Ω m), (3) very low resistivity unit (10–40 Ω m) expanding from the summit area, (4) buried low resistivity channel (30–100 Ω m), (5) massive lava flows (> 400 Ω m), (6) perched aquifer (30–100 Ω m) (7) Undifferentiated, unsaturated weathered basaltic rocks (100–400 Ω m). The shading with depth reflects the approximative depth of investigation.

3.2 Results

Resistivities of the 4-layer 3-D model range between ca. 1 and 3000 Ω m. The depth of penetration was approximated from the depth to the last geophysical interface, i.e. between the 3rd and 4th resistivity layers, and ranged between 20 and 550 m with a mean of 165 m b.g.l. (below ground level).

3.2.1 Contrasts between the windward and leeward sides

The geophysical survey reveals a striking contrast in resistivity between the windward and leeward sides of San Cristóbal Island (Figs. 4 and 5). Above sea level, the subsurface of the northern side is resistive (800–3000 Ω m), which is compatible with unweathered, unsaturated basaltic rocks (Descloitres et al., 1997, 2000). In contrast, the bulk of the southern, windward side presents low to intermediate resistivity (10–200 Ω m), compatible with basaltic rocks subject to various degrees of weathering or saturation (Descloitres et al., 1997; Lénat et al., 2000; Müller et al., 2002).

No constructional process can be invoked to explain such a contrast between the windward and leeward sides. Erupted lavas and pyroclastic deposits of the two sides shared identical chemical and physical properties at the date of their emplacement (Geist et al., 1986). A difference that could be expected between the two sides of the island is a higher amount of volcanic ash blown by the trade-winds to the north. But these materials are easily weathered and would reduce resistivity in the north, contrary to what is observed.

The contrast in resistivity can therefore be explained by differential weathering induced by the contrasting climatic conditions at the surface and the presence of groundwater in the subsurface. Weathering confers a low resistivity to basaltic rocks due to the presence of clayey secondary minerals (Eggleton et al., 1987; Gislason et al., 1993). As weathering rates are enhanced by water percolation, areas with higher recharge rates are prone to enhanced rock weathering (Adelinet et al., 2008; Gislason et al., 1993; Hay and

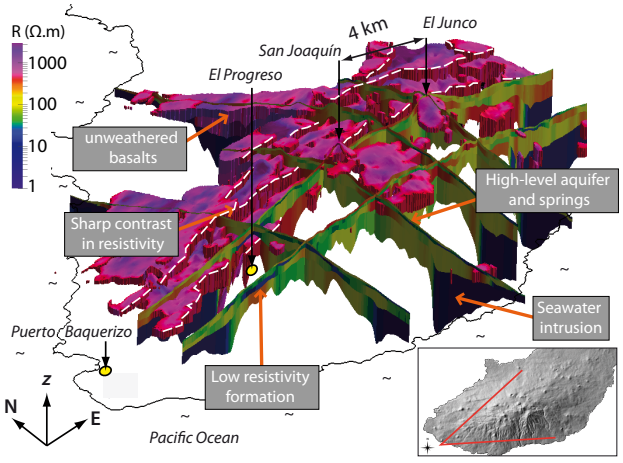

Fig. 5. 3-D view of the SkyTEM 4-layer resistivity model. The high resistivity extraction (threshold of resistivity $> 400\,\Omega$m) reveals sharp transitions in resistivity. The edges of the high resistivity extraction (white, dashed lines) correspond to the boundaries of the buried low-resistivity channel (Sect. 3.2.4). These edges are aligned with eruptive cones at the surface, which suggests the alignement with a dyke swarm.

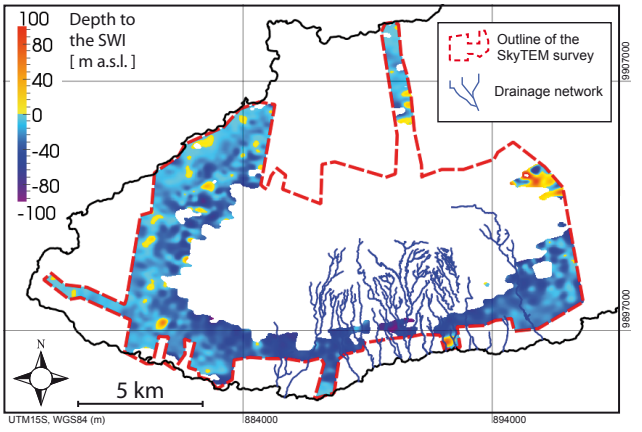

Fig. 6. Depth to the saltwater interface (SWI) inferred from the 4 layer resistivity model. SWI elevation is estimated from the elevation of the upper interface of the deep, very conductive geophysical layers ($< 15\,\Omega$m). Values a.s.l. are artefacts and should be disregarded.

Jones, 1972; Van der Weijden and Pacheco, 2003). Similarly to the neighbouring Santa Cruz Island (d'Ozouville et al., 2008), contrasting climatic conditions in San Cristóbal induce marked differences in rock weathering between the windward and leeward sides.

3.2.2 Imprints of saltwater intrusion

Cross-sections (Fig. 4) reveal a very conductive unit (1–15 Ωm) standing close to, or below, sea level around the central shield. This is the typical signature of seawater intrusion beneath a basal aquifer (Auken et al., 2009b), which is confirmed by field observation. The aquifer outcrops at the bottom of a pit mine near Puerto Baquerizo (Fig. 1) and the water is brackish ($\chi = 28$ mS cm^{-1}).

A map of the saltwater interface (SWI) was derived from the elevation of the upper interface of the lower, very conductive ($< 15\,\Omega$m) geophysical layer (Fig. 6). This SWI map provides only an estimate, as the actual interface between sea- and freshwater is often diffused, and vertical salinity profiles measured in monitoring wells are necessary to better define the actual thickness of the freshwater lens (Izuka and Gingerich, 1998). The SWI appears shallower on the dry northern and western slopes (0–30 m b.s.l. – below sea level) and deeper at the southern windward side (0–100 m b.s.l.). The SWI is particularly deep at the center of the southern watershed, 1.6 km from the coast, where surface drainage network concentrates (Fig. 6). In the central part of the surveyed area, the SWI is too deep with respect to ground level to be detected by SkyTEM soundings.

The freshwater lens could not be resolved with the 4-layer inversion model, but an estimate of the water table elevation can be inferred from the SWI map (Lienert, 1991). Assuming hydrostatic equilibrium and no mixing between fresh- and saltwater, the Ghyben-Herzberg equation relates the elevation of the water table to the SWI depth by a ratio of 1 to 40 (see e.g. Bear, 1999). This method is not accurate, but provides an order of magnitude of the water table elevation (Izuka and Gingerich, 1998). At the windward side of the island, the depth to the SWI is estimated to range between 0 and 100 m b.s.l. (Fig. 6). This yields a water table ranging only between 0 and 2.5 m a.s.l..

3.2.3 High-level groundwater

Numerous springs identified at the surface are located below outcrops of weakly resistive geophysical layers (30–100 Ωm, greenish colors, Fig. 4). As spring water is poorly mineralized ($\chi = 30$ to 170 µS cm^{-1}), the presence of groundwater cannot explain alone the observed low rock electrical resistivities. The low resistivity is attributed to the occurrence of clayey minerals, produced by the alteration of basaltic rocks (Eggleton et al., 1987; Gislason et al., 1993).

As shown in Sect. 3.2.2, the basal aquifer water table remains at low elevation (0–2.5 m a.s.l.) up to 1.7 km from the coast. The basal aquifer is therefore unlikely to be at the origin of the springs located at ca. 150 m a.s.l., 2 km from the coastline. High-level springs must originate from perched aquifers, disconnected from the basal aquifer, as proposed, e.g. for Hawaii (Ingebritsen and Scholl, 1993), Réunion (Join et al., 1997; Violette et al., 1997), and Cape Verde (Heilweil et al., 2009) islands. Perched aquifers can form over impervious units, e.g. ash deposits, and red "baked" soils, which

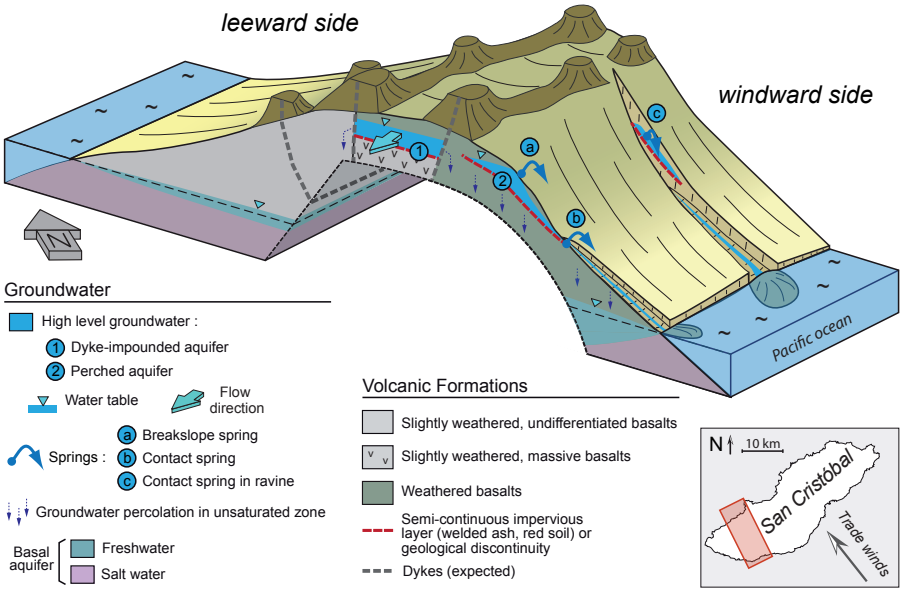

Fig. 7. Hydrogeological conceptual model of San Cristóbal Island, inferred from geomorphological observations and airborne electromagnetic survey. The configuration is asymmetric, the basal aquifer is thin and basalt are weakly weathered in the northern leeward side, while the basal aquifer is thicker and basalts are weathered in the southern, windward side. Springs are fed by perched aquifers and a dyke-impounded aquifer may be present in the central area.

are too thin to be resolved with TEM soundings, but have been identified on coastal cliffs and ravines of San Cristóbal (Fig. 3c).

3.2.4 Low resistivity channel

In the summit zone, subsurface resistive units of the northern side give place southward to a low-resistivity (30–100 Ω m), WSW–ENE trending buried channel (Figs. 4 and 5). This low resistivity channel is located between 10–100 m b.g.l., and locally outcrops without notable difference at the surface. Sharp contrasts in resistivity are highlighted by thick (up to 100 m) vertical edges in the high-resistivity extraction (Fig. 5). Furthermore, the edges of the high-resistivity extraction are aligned with volcanic cones at the surface, which can reveal the presence of a WSW–ENE trending dyke swarm (Fig. 2, black dashed lines). Such an alignment is less conspicuous for the southern offset.

The presence of low resistivity units in the central areas of volcanic islands is often associated with hydrothermally altered rocks (Aizawa et al., 2009; Müller et al., 2002; Revil et al., 2004), but there is no evidence of past or present hydrothermal activity on San Cristóbal. A resistivity of 30–100 Ω m is compatible with saturated, weathered basaltic rocks (see Sect. 3.2.3), and the central, buried low-resistivity channel can be interpreted as a dyke-impounded aquifer, which is commonly observed in other volcanic islands (Custodio, 2004; Stearns and McDonald, 1947; Takasaki and Mink, 1981). As detailed by Bret et al. (2003) from observations performed in a horizontal tunnel in La Reunion Island, the occurrence of a dyke-impounded aquifer can induce sharp contrast in rock weathering. Such a phenomenon can be invoked to explain the sharp transition in resistivity observed in the summit zone of San Cristóbal.

The central low-resistivity channel dips westward and terminates, expanding over the southwestern flank of the main shield with decreasing resistivities (10–40 Ω m) (Fig. 4a, b, CS1-No. 3). This unit is subparallel to the topography and seems to circumvent volcanic cones. Such a low resistivity unit may be interpreted as the effect of enhanced weathering induced by groundwater flow from the dyke-impounded aquifer. Yet, the resistivities are particularly low and may reveal distinct geological units such as older lava flows, or colluvial deposits with high clay content.

4 Discussion

4.1 Hydrogeological conceptual model

We define the first hydrogeological conceptual model of San Cristóbal Island (Fig. 7). The freshwater lens is thicker at the windward side, but the water table remains at low elevation (ca. 0–2.5 m a.s.l.). As a consequence, the basal aquifer cannot be invoked to explain the occurrence of springs at high elevation (Sect. 3.2.2). Springs are more likely associated with perched aquifers developing over impervious layers, such as red "baked" soils (Sect. 3.2.3). The buried low-resistivity channel revealed in the summit zone can be interpreted as a dyke-impounded aquifer (Sect. 3.2.4).

This hydrogeological configuration, often referred to as the Hawaiian model in the literature (Custodio, 2004; Stearns and McDonald, 1947), has been identified in similar volcanic islands such as Hawaii, Azores, and Réunion (Cruz and França, 2006; Ingebritsen and Scholl, 1993; Violette et al., 1997; Join et al., 1997).

4.2 Resistivity mapping in basaltic environments

On the basis of a study on small rock samples, Perrier and Froidefond (2003) showed that the electrical properties of volcanic rocks are mainly controlled by secondary minerals. The contrast in resistivity between the windward and leeward sides of San Cristóbal Island also illustrates this result: marked differences in resistivity between the two sides are interpreted as the consequence of differential weathering (Sect. 3.2.1).

These results highlight that resistivity mapping in volcanic environments may result in the mapping of weathering. In this context, the identification of freshwater saturation remains ambiguous. The occurrence of fresh groundwater can yet be detected indirectly, since the water table often corresponds to a contrast in rock weathering (Keller et al., 1979; Lienert, 1991). On San Cristóbal Island, for instance, the presence of clayey minerals in the saturated levels explains that perched aquifers at the origin of springs are associated with particularly low resistivities (30–100 Ω m), though groundwater is poorly mineralized (30 and 170 μS cm^{-1}).

This study shows that exploratory AEM surveys are efficient for resistivity imaging over large inaccessible areas. In volcanic islands, the implementation of AEM survey allows an efficient mapping of intruding saltwater and weathered rocks, that are both characterized by low resistivities. The geometry of freshwater aquifers may be inferred from resistivity maps, but their resistivity signature depends on the degree of weathering of the host rocks. As a consequence, the definition of an hydrogeological conceptual model requires additional field observations.

5 Conclusions

The SkyTEM survey conducted over San Cristóbal Island provides a map of resistivity over 140 km^2 with a mean penetration depth of 165 m b.g.l. The survey reveals a marked contrast in subsurface resistivity between the windward and leeward sides, which is explained by differential weathering induced by contrasting climatic conditions at the surface. Combined with remote sensing and geomorphological observations, geophysical data provides valuable insights into the hydrogeological settings. The first hydrogeological conceptual model is proposed for San Cristóbal Island, it can be related to the Hawaiian model for volcanic islands: a basal aquifer subject to seawater intrusion, a series of perched aquifers, and a dyke impounded aquifer in the summit zone. The hydrogeological conceptual model can now be validated with land-based geophysical surveys directly sensitive to groundwater occurrence (proton magnetic resonance, self-potential) and a drilling campaign focused in the areas of interest.

Acknowledgements. This study was performed within the framework of the project Galapagos Islands Integrated Water Studies (GIIWS), funded by the Agence Nationale de la Recherche (ANR-blanc 2010 GIIWS Ref. 601–01). The Charles Darwin Research Station and the Galapagos National Park collaborated with the 2006 SkyTEM survey in Galápagos, which was funded by Foundation de France, Foundation Véolia Environnement, Fondation Schlumberger-SEED, Chancellerie des Universités de Paris, UGAFIP-BID and the Municipality of Santa Cruz. The authors would like to thank David Fauchet, Wafa Ramdani and Fabian Lindner for their participation in the digitalization of cones, fractures and rivers, which was performed under Qgis (http://www.qgis.org). Finally, the helpful comments and corrections by D. Geist and another anonymous reviewer are gratefully acknowledged.

Edited by: Y. Fan

References

Acocella, V. and Neri, M.: Dike propagation in volcanic edifices: overview and possible developments, Tectonophysics, 471, 67–77, 2009.

Adelinet, M.: Etude hydrologique des bassins versants de l'île de San Cristóbal (Galapagos, Equateur), Master's thesis, ENS Paris and UPMC Sisyphe Lab., Univ. Paris 6, 2005.

Adelinet, M., Fortin, J., d'Ozouville, N., and Violette, S.: The relationship between hydrodynamic properties and weathering of soils derived from volcanic rocks, Galapagos Islands (Ecuador), Environ. Geol., 56, 45–58, 2008.

Aizawa, K., Ogawa, Y., and Ishido, T.: Groundwater flow and hydrothermal systems within volcanic edifices: delineation by electric self-potential and magnetotellurics, J. Geophys. Res.-Sol. Ea., 114 , B01208, doi:10.1029/2008JB005910, 2009.

Auken, E., Christiansen, A., Westergaard, J., Kirkegaard, C., Foged, N., and Viezzoli, A.: An integrated processing scheme for high-resolution airborne electromagnetic surveys, the SkyTEM system, Explor. Geophys., 40, 184–192, 2009a.

Auken, E., Violette, S., d'Ozouville, N., Deffontaines, B., Sørensen, K., Viezzoli, A., and de Marsily, G.: An integrated study of the hydrogeology of volcanic islands using helicopter borne transient electromagnetic: application in the Galapagos Archipelago, C. R. Geosci., 341, 899–907, 2009b.

Bardintzeff, J. and McBirney, A.: Volcanology, Jones and Barlett, London, 1–269, 2006.

Bear, J.: Conceptual and mathematical modeling, in: Seawater Intrusion in Coastal Aquifers: Concepts, Methods, and Practices, Springer, 163–191, 1999.

Bosch, J., Bakker, M. J., Gunnink, J., and Paap, B.: Airborne electromagnetic measurements as basis for a 3-D geological model of an elsterian incision, Z. Dtsch. Ges. Geowiss., 160, 249–258, 2009.

Bret, L., Join, J., Legal, X., Coudray, J., and Fritz, B.: Clays and zeolites in the weathering of a basaltic tropical shield volcano (Le Piton des Neiges, Reunion Island), C. R. Geosci., 335, 1031–1038, 2003.

Chadwick, W. and Howard, K.: The pattern of circumferential and radial eruptive fissures on the volcanoes of Fernandina and Isabela islands, Galapagos, B. Volcanol., 53, 259–275, 1991.

Colinvaux, P.: Climate and the Galapagos islands, Nature, 240, 17–20, 1972.

Cox, A.: Paleomagnetism of San Cristóbal Island, Galapagos, Earth Planet. Sc. Lett., 11, 152–160, 1971.

Cruz, J. and França, Z.: Hydrogeochemistry of thermal and mineral water springs of the Azores archipelago (Portugal), J. Volcanol. Geoth. Res., 151, 382–398, 2006.

Custodio, E.: Hydrogeology of volcanic rocks, in: Hydrogeology of Volcanic Rocks, UNESCO, Paris, 395–425, 2004.

Descloitres, M., Ritz, M., Robineau, B., and Courteaud, M.: Electrical structure beneath the eastern collapsed flank of Piton de la Fournaise volcano, Reunion Island: implications for the quest for groundwater, Water Resour. Res., 33, 13–19, 1997.

Descloitres, M., Guérin, R., Albouy, Y., Tabbagh, A., and Ritz, M.: Improvement in TDEM sounding interpretation in presence of induced polarization. A case study in resistive rocks of the Fogo volcano, Cape Verde Islands, J. Appl. Geophys., 45, 1–18, 2000.

Eggleton, R., Foudoulis, C., and Varkevisser, D.: Weathering of basalt: changes in rock chemistry and mineralogy, Clay. Clay Miner., 35, 161–169, 1987.

Falkland, A.: Tropical island hydrology and water resources current knowledge and future needs, in: hydrology and water management in the humid tropics, Proceedings of the second International Colloquium, Panama, 237–349, 1999.

Falkland, A. and Custodio, E.: Guide on the hydrology of small islands. studies and reports in hydrology, UNESCO, Paris, Vol. 49, 51–130, 1991.

Fetter, C.: Applied hydrogeology, Prentice Hall, Upper Saddle River, New Jersey, USA, 1994.

Finn, C., Sisson, T., and Deszcz-Pan, M.: Aerogeophysical measurements of collapse-prone hydrothermally altered zones at Mount Rainier volcano, Nature, 409, 600–603, 2001.

Finn, C., Deszcz-Pan, M., Anderson, E., and John, D.: Three-dimensional geophysical mapping of rock alteration and water content at Mount Adams, Washington: implications for lahar hazards, J. Geophys. Res.-Sol. Ea., 112, B10204, doi:10.1029/2006JB004783, 2007.

Geist, D., McBirney, A., and Duncan, R.: Geology and petrogenesis of lavas from San Cristóbal Island, Galapagos Archipelago, Bull. Geol. Soc. Am., 97, 555–566, 1986.

Gingerich, S. B. and Oki, D. S.: Ground Water in Hawaii, Tech. rep., USGS Pacific Islands Water Science Center, http://pubs.usgs.gov/fs/2000/126/ (last access: August 2012), USGS, Honolulu, Hawaii, 2000.

Gislason, S., Veblen, D., and Livi, K.: Experimental meteoric water-basalt interactions: characterization and interpretation of alteration products, Geochim. Cosmochim. Ac., 57, 1459–1471, 1993.

Gómez-Ortiz, D., Martín-Velázquez, S., Martín-Crespo, T., Márquez, A., Lillo, J., López, I., Carreño, F., Martín-González, F., Herrera, R., and De Pablo, M.: Joint application of ground penetrating radar and electrical resistivity imaging to investigate volcanic materials and structures in Tenerife (Canary Islands, Spain), J. Appl. Geophys., 62, 287–300, 2007.

Hay, R. and Jones, B.: Weathering of basaltic tephra on the island of Hawaii, Geol. Soc. Am. Bull., 83, 317–332, 1972.

Heilweil, V. M., Solomon, D. K., Gingerich, S. B., and Verstraeten, I. M.: Oxygen, hydrogen, and helium isotopes for investigating groundwater systems of the Cape Verde Islands, West Africa, Hydrogeol. J., 17, 1157–1174, 2009.

Ingebritsen, S. and Scholl, M.: The hydrogeology of Kilauea volcano, Geothermics, 22, 255–270, 1993.

Ingala, Orstom and Pronareg: Inventario Cartográfico de los Recursos Naturales, Geomorfología, Vegetacón, Hidricos, Ecológicos y Biofisicos de las Islas Galápagos Ecuador, Ingala, Quito, Ecuador, 1987.

IPCC: Contribution of working groups I, II and III to the fourth assessment report of the intergovernmental panel on climate change, 104, Chapter: Climate change and its impacts in the near and long term under different scenarios, IPCC, Geneva, Switzerland, 43–54, 2007.

Izuka, S. and Gingerich, S.: Estimation of the depth to the freshwater/salt-water interface from vertical head gradients in wells in coastal and island aquifers, Hydrogeol. J., 6, 365–373, 1998.

Join, J., Coudray, J., and Longworth, K.: Using principal components analysis and Na/Cl ratios to trace groundwater circulation in a volcanic island: the example of Reunion, J. Hydrol., 190, 1–18, 1997.

Keller, G., Grose, L., Murray, J., and Skokan, C.: Results of an experimental drill hole at the summit of Kilauea volcano, Hawaii, J. Volcanol. Geoth. Res., 5, 345–385, 1979.

Lénat, J., Fitterman, D., Jackson, D., and Labazuy, P.: Geoelectrical structure of the central zone of Piton de la Fournaise volcano (Réunion), B. Volcanol., 62, 75–89, 2000.

Lienert, B.: An electromagnetic study of Maui's last active volcano, Geophysics, 56, 972–982, 1991.

MacNeil, R., Sanford, W., Connor, C., Sandberg, S., and Diez, M.: Investigation of the groundwater system at Masaya Caldera, Nicaragua, using transient electromagnetics and numerical simulation, J. Volcanol. Geoth. Res., 166, 217–232, 2007.

Mogi, T., Kusunoki, K., Kaieda, H., Ito, H., Jomori, A., Jomori, N., and Yuuki, Y.: Grounded Electrical-source Airborne Transient Electromagnetic (GREATEM) survey of Mount Bandai, North-Eastern Japan, Explor. Geophys., 40, 1–7, 2009.

Müller, M., Hördt, A., and Neubauer, F.: Internal structure of Mount Merapi, Indonesia, derived from long-offset transient electromagnetic data, J. Geophys. Res.-Sol. Ea., 107, 2187, doi:10.1029/2001JB000148, 2002.

Mullen, I., Wilkinson, K., Cresswell, R., and Kellett, J.: Three-dimensional mapping of salt stores in the Murray-Darling Basin, Australia: 2. Calculating landscape salt loads from airborne electromagnetic and laboratory data, Int. J. Appl. Earth Obs., 9, 103–115, 2007.

d'Ozouville, N.: Agua Dulce, La realidad de un recurso crítico, in: Informe Galápagos 2006–2007, Puerto Ayora, Galápagos, Ecuador, 2007a.

d'Ozouville, N.: Etude du Fonctionnement Hydrologique Dans les Iles Galápagos : caractérisation d'un milieu volcanique insulaire et préalable à la gestion de la ressource., Ph. D. thesis, Université Paris 6 Pierre et Marie Curie, 2007b.

d'Ozouville, N., Auken, E., Sorensen, K., Violette, S., de Marsily, G., Deffontaines, B., and Merlen, G.: Extensive perched aquifer and structural implications revealed by 3-D resistivity mapping in a Galapagos volcano, Earth Planet. Sc. Lett., 269, 517–521, 2008.

Perrier, F. and Froidefond, T.: Electrical conductivity and streaming potential coefficient in a moderately alkaline lava series, Earth Planet. Sc. Lett., 210, 351–363, 2003.

Pryet, A.: Hydrogeology of Volcanic Islands: a Case-Study in the Galapagos Archipelago, Ph. D. thesis, Université Pierre et Marie Curie, Paris, 2011.

Pryet, A., Ramm, J., Chilès, J.-P., Auken, E., Deffontaines, B., and Violette, S.: 3-D resistivity gridding of large AEM datasets: A step toward enhanced geological interpretation, J. Appl. Geophys., 75, 277–283, 2011.

Pryet, A., Dominguez, C., Fuente Tomai, P., Chaumont, C., d'Ozouville, N., Villacís, M., and Violette, S.: Quantification of cloud water interception along the windward slope of Santa Cruz Island, Galapagos, Agr. Forest Meteorol., 161, 94–106, 2012.

Rabus, B., Eineder, M., Roth, A., and Bamler, R.: The shuttle radar topography mission – a new class of digital elevation models acquired by spaceborne radar, Int. Soc. Photogramme., 57, 241–262, 2003.

Revil, A., Finizola, A., Sortino, F., and Ripepe, M.: Geophysical investigations at Stromboli Volcano, Italy: implications for ground water flow and paroxysmal activity, Geophys. J. Int., 157, 426–440, 2004.

Siemon, B.: Levelling of helicopter-borne frequency-domain electromagnetic data, J. Appl. Geophys., 67, 206–218, 2009.

Simkin, T.: Geology of Galapagos, Biol. J. Linn. Soc., 21, 61–75, 1984.

Singhal, B. and Gupta, R.: Hydrogeology of volcanic rocks, in: Applied Hydrogeology of Fractured Rocks, Springer Netherlands, 257–268, 2010.

Sørensen, K. and Auken, E.: SkyTEM–A new high-resolution helicopter transient electromagnetic system, Explor. Geophys., 35, 191–199, 2004.

Stearns, H. and McDonald, G.: Geology and groundwater resources of the island of Hawaii, Hawaii Division of Hydrography Bulletin, 9, p. 363, 1947.

Steuer, A., Siemon, B., and Auken, E.: A comparison of helicopter-borne electromagnetics in frequency- and time-domain at the Cuxhaven valley in Northern Germany, J. Appl. Geophys., 67, 194–205, 2009.

Supper, R., Motschka, K., Ahl, A., Bauer-Gottwein, P., Gondwe, B., Alonso, G., Romer, A., Ottowitz, D., and Kinzelbach, W.: Spatial mapping of submerged cave systems by means of airborne electromagnetics: an emerging technology to support protection of endangered karst aquifers, Near Surf. Geophys., 7, 613–627, 2009.

Takasaki, K. and Mink, J.: Evaluation of Major Dike-impounded Ground-water Reservoirs, Island of Oahu, US Department of the Interior, Geological Survey, US Geological Survey water-supply paper 2217, Honolulu, Hawaii, 1981.

Trueman, M. and d'Ozouville, N.: Characterizing the Galapagos terrestrial climate in the face of global climate change, Galapagos Res., 67, 26–37, 2010.

Underwood, M. R., Peterson, F. L., and Voss, C. I.: Groundwater lens dynamic of atoll islands, Water Resour. Res., 28, 2889–2902, 1992.

Van der Weijden, C. and Pacheco, F.: Hydrochemistry, weathering and weathering rates on Madeira Islands, J. Hydrol., 283, 122–145, 2003.

Viezzoli, A., Christiansen, A. V., Auken, E., and Sorensen, K.: Quasi-3-D modeling of airborne TEM data by spatially constrained inversion, Geophysics, 73, 105–113, 2008.

Viezzoli, A., Munday, T., Auken, E., and Christiansen, A.: Accurate quasi 3-D versus practical full 3-D inversion of AEM data, Preview, 149, 23–31, 2010a.

Viezzoli, A., Tosi, L., Teatini, P., and Silvestri, S.: Surface water–groundwater exchange in transitional coastal environments by airborne electromagnetics: the Venice Lagoon example, Geophys. Res. Lett., 37, L01402, doi:10.1029/2009GL041572, 2010b.

Violette, S., Ledoux, E., Goblet, P., and Carbonnel, J.: Hydrologic and thermal modeling of an active volcano: the Piton de la Fournaise, Reunion, J. Hydrol., 191, 37–63, 1997.